Sepsis induces brain mitochondrial dysfunction

Joana da Costa P. d'Avila, MS; Ana Paula S. A. Santiago, MS; Rodrigo T. Amâncio, MD; Antonio Galina, PhD; Marcus F. Oliveira, PhD; Fernando A. Bozza, MD, PhD

Objective: **Mitochondrial dysfunctions have been associated with the pathogenesis of sepsis. A systematic survey of mitochondrial function in brain tissues during sepsis is lacking. In the present work, we investigate brain mitochondrial function in a septic mouse model.**

Design: **Prospective animal study.**

Setting: **University research laboratory.**

Subjects: **Male Swiss mice, aged 6–8 wks.**

Interventions: **Mice were subjected to cecal ligation and perforation (sepsis group) with saline resuscitation or to sham operation (control group).**

Measurements and Main Results: **Oxygen consumption was measured polarographically in an oximeter. Brain homogenates from septic animals presented higher oxygen consumption in the absence of adenosine 5'-diphosphate (state 4) compared with control animals. The increase in state 4 respiration in animals in the cecal ligation and perforation group resulted in a drastic decrease in both respiratory control and adenosine 5'-diphosphate/oxygen ratios, indicating a reduction in the oxidative phosphorylation efficiency. Septic animals presented a significant increase in the recovery time of mitochondrial membrane potential on adenosine 5'-diphosphate addition compared with control animals, suggesting a proton leak through the inner mitochondrial membrane. The septic group presented a general reduction in the content of cytochromes. Moreover, the activity of cytochrome *c* oxidase was specifically and significantly decreased in the brain during sepsis. Hydrogen peroxide generation by brain mitochondria from septic mice did not respond to substrates of electron transport chain or to adenosine 5'-diphosphate, showing that mitochondrial function may be compromised in a critical level in the brain during sepsis.**

Conclusions: **The mitochondrial dysfunctions demonstrated here indicate that uncoupling of oxidative phosphorylation takes place in the brain of septic mice, compromising tissue bioenergetic efficiency. (Crit Care Med 2008; 36:1925–1932)**

KEY WORDS: energy metabolism; MODS; mitochondria; sepsis; brain; oxidative stress

The evolution to multiorgan dysfunction syndrome is a critical determinant of mortality in septic patients, and the mechanisms by which sepsis leads to organ dysfunction remain to be established. Tissue hypoxia has long been considered the putative mechanism of multiorgan dysfunction syndrome (1). In recent decades, there has been an intense controversy about the benefits of tissue oxygen delivery strategies during sepsis (2–4), and recently, it has been shown that early intervention aimed at increasing tissue oxygen delivery improves the outcome of septic patients (5).

Although the determinants of tissue metabolic demands in early sepsis are not completely known, there is strong evidence indicating that mitochondrial function is affected during sepsis (6, 7). The functional changes in mitochondria may be, ultimately, a consequence of either electron transport chain impairment or loss of the membrane potential, which may contribute to organ injury and cell death (8–12).

During sepsis, the brain is one of the first organs to be affected, and sepsis-associated encephalopathy is frequent but infrequently recognized (13, 14). An encephalopathy of variable severity has been found to occur in 9% to 71% of septic patients and is associated with higher in-hospital mortality (15, 16). In addition, *post mortem* analysis of septic patients revealed a high frequency of brain lesions (17). In animal models of polymicrobial sepsis, acute encephalopathy takes place, and survivors present with cognitive impairment that could be secondary to central nervous system damage (18). There is evidence suggesting that short-term oxidative damage in brains of rats subjected to cecal ligation and perforation (CLP) could contribute to the development of central nervous system symptoms during the progression of sepsis (19). In fact, brain tissues have unique characteristics that make them especially susceptible to damage during sepsis, such as their high oxygen consumption rate and low levels of antioxidant defenses (20).

Thus, in the present work, we investigated mitochondrial function in the

From the Laboratório de Bioquímica Redox, Programa de Biologia Molecular e Biotecnologia (JdCPdA, MFO), Laboratório de Bioenergética Adaptativa, Programa de Biofísica e Bioquímica Celular (APSAS, AG), Instituto de Bioquímica Médica, Universidade Federal do Rio de Janeiro, Cidade Universitária, Rio de Janeiro, Brazil; and the Instituto de Pesquisa Clínica Evandro Chagas and Laboratório de Imunofarmacologia, Instituto Oswaldo Cruz, Fiocruz, Rio de Janeiro, Brazil (RTA, FAB).

The authors have not disclosed any potential conflicts of interest.

Supported, in part, by grants from Conselho Nacional de Desenvolvimento Científico e Tecnológico (CNPq, Brazil) and DECIT/Ministério da Saúde (MS) through Edital Acidentes e Trauma 2004, CNPq through Edital Universal 2003 and 2006, Fundação Universitáriã José Bonifácio (FUJB, Brazil) through Prêmio Antônio Luiz Vianna 2004 and Fundação Carlos Chagas Filho de Amparo à Pesquisa do Estado do Rio de Janeiro (FAPERJ, Brazil) through APQ-1 and Fundação Oswaldo Cruz - PAPES IV (Brazil). Drs. Oliveira and Galina are research scholars from CNPq.

Drs. Oliveira and Bozza contributed equally to this work.

For information regarding this article, E-mail: maroli@bioqmed.ufrj.br *or* fbozza@hucff.ufrj.br

DOI: 10.1097/CCM.0b013e3181760c4b

brains of septic mice. The data presented here support the notion that during sepsis, an increase in proton permeability across the inner mitochondrial membrane takes place in the brain, reducing the efficiency of oxidative phosphorylation due to mitochondrial uncoupling.

MATERIALS AND METHODS

Animals. Male Swiss mice (Oswaldo Cruz Foundation breeding unit) weighing 20–25 g were used. The animals were kept at a constant temperature (25°C), with free access to pelleted diet and water in a room with a 12-hr light/dark cycle. Animals were maintained according to international and local animal care guidelines. The present protocol was approved by the Oswaldo Cruz Foundation Animal Welfare Committee.

Cecal Ligation and Perforation. CLP was performed as previously described, with minor modifications (21, 22). Briefly, male Swiss mice were anesthetized with ketamine (80 mg/kg, Ketamin, Cristália) and thiopental (30 mg/kg, Thiopental, Cristália) diluted in sterile saline and administered intraperitoneally (0.2 mL). Laparotomy was performed with a 2-cm midline incision through the linea alba; the cecum was exposed and carefully ligated with sterile 3-0 silk below the ileocecal junction, with care to avoid bowel obstruction. The cecum was punctured once with an 18-gauge needle and was then gently squeezed to empty its content through the puncture. The cecum was then returned to the peritoneal cavity, and the abdominal muscle and skin incisions were closed in layers using a 3-0 nylon suture line. Immediately after the surgery, 0.5 mL of sterile saline was administered subcutaneously to the animals for volume resuscitation. Mice in the sham operation group were subjected to identical procedures, except that ligation and puncture of the cecum were omitted. Animals subjected to CLP developed early signs of sepsis, including lethargy, piloerection, and diarrhea. The lethality of our model was about 40% in the first 24 hrs and 60% in 144 hrs (22). After 24 hrs, CLP mice were killed by cervical dislocation, and brain tissues were obtained.

Preparation of Brain Homogenates. Brains were removed, rinsed with ice-cold homogenate buffer (10 mM Tris buffer pH 7.4, 0.32 M sucrose, and 1 mM EGTA), minced, and manually homogenized in a 30-mL Teflon glass potter with a volume of buffer adjusted to provide a 10% (wt/vol) final concentration (typically 4 mL) as previously described (23). All procedures were performed on ice. Protein content was determined by the Folin–Lowry method using bovine serum albumin as standard (24).

Mitochondria Isolation. Mitochondria were isolated from brain homogenates using a method previously described in the literature (25). The homogenate was centrifuged for 3 mins at 4,000 rpm in a Hitachi Himac SCR20B RPR 20-2 rotor to remove cell debris. After centrifugation, the supernatant was centrifuged for 10 mins at 16,000 rpm. The pellet was resuspended in 5 mL of homogenate buffer containing 15% Percoll and a discontinuous gradient was prepared with 40% under 23% and 15% Percoll. The gradient was centrifuged at 19,000 rpm for 5 mins, and the mitochondrial fraction between 40% and 23% was collected and centrifuged at 14,000 rpm for 10 mins to wash the Percoll. The pellet was suspended in ice-cold homogenate buffer modified with 0.32 M mannitol instead of sucrose, plus 0.2% bovine serum albumin, fatty acid free. Mitochondria preparation was kept at 4°C during the whole isolation procedure, and protein was determined by the Folin-Lowry method, using bovine serum albumin as a standard (24).

Oxygen Consumption Measurements. Oxygen concentrations in the medium were measured polarographically using an oximeter fitted with a water-jacketed, Clark-type electrode (Yellow Springs Instrument 5300) in a 1.5-mL reaction vessel. Oxygen consumption studies were carried out in a respiration buffer (10 mM Tris-HCl, pH 7.4, 0.32 M mannitol, 5 mM inorganic phosphate, 50 mM KCl, 4 mM $MgCl_2$, 1 mM EGTA) modified from the literature (23). Samples of brain homogenates (650 μg/mL) were incubated with respiration buffer inside the oximeter cuvette under stirring. State 3 respiration was induced by addition of Complex I substrates pyruvate (10 mM) and malate (10 mM), plus 100 μM adenosine 5'-diphosphate (ADP) to the closed cuvette using a Hamilton syringe. State 4 respiration was reached when all ADP was metabolized to adenosine triphosphate (ATP). Then, after the first induction of state 4 respiration, 200 μM ADP was added to the cuvette, stimulating oxygen consumption during state 3, which was followed by a second state 4 respiration. Respiratory control ratio values were obtained by dividing the rate of oxygen consumption at state 3 by the rate of oxygen consumption at state 4 (26). After a stable state 4 respiration, the addition of 5 μM carbonyl cyanide p-(trifluoromethoxy)phenylhydrazone (FCCP) induced a maximal uncoupled response.

Determination of Mitochondrial Membrane Potential. Mitochondrial membrane potential ($\Delta\Psi m$) was measured by using the cationic dye safranine O (Sigma), which accumulates inside the negatively charged mitochondrial matrix and quenches its fluorescence signal (27). Mitochondria (0.3 mg protein/mL) were incubated in the standard respiration buffer supplemented with 10 μM safranine. FCCP (5 μM) was used as a positive control to collapse $\Delta\Psi m$. Fluorescence was detected with an excitation wavelength of 495 nm (slit 5 nm) and an emission wavelength of 586 nm (slit 5 nm) using a Hitachi (Tokyo, Japan) model F-3010 spectrofluorometer. Data are reported as arbitrary fluorescence units. Each experiment was repeated at least three times with different mitochondrial preparations isolated from Percoll gradient centrifugation (25).

Visible Absorption Spectra of Mitochondrial Cytochromes. Estimations of cytochrome content were carried out in brain homogenates by using a GBC spectrophotometer (UV/VIS 920) at 1 sec of integration time and data recording at each 0.85-nm interval. Homogenate protein (0.2 mg) from sham and CLP brains was incubated in a 100 mM phosphate buffer containing 0.1% Triton X-100, and the absorption light wavelength scan of cytochromes was performed (oxidized) between 500 and 700 nm. Sodium dithionite was added to the cuvette, and differential spectra (reduced minus oxidized) were calculated in the GBC Spectral Software (GBC, Australia).

Electron Transport Chain Complex Activities. The mitochondrial Complexes I–III and IV activities were determined, as described previously in the literature (28, 29), at 37°C. For nicotinamide adenine dinucleotide (NADH)–cytochrome-*c* reductase (Complexes I–III) activity, brain homogenates were briefly centrifuged for 10 secs to clarify the sample, protein content was determined, and the samples were kept at −80°C until analysis. The sample (about 0.3 mg of protein) was added to 100 mM phosphate buffer containing 50 μM cytochrome c^{3+} and 1 mM potassium cyanide and the rotenone-sensitive NADH-cytochrome-*c* reductase activity was determined at 550 nm. For cytochrome *c* oxidase (Complex IV) activity, sample (about 0.3 mg of protein) was added to an oximeter cuvette, the potassium cyanide–sensitive oxygen consumption induced by tetramethylparaphenylinediamine (0.5 mM), and ascorbate (5 mM) was determined.

Hydrogen Peroxide Production in Brain Homogenates. Hydrogen peroxide (H_2O_2) production was measured using Amplex Red (Molecular Probes) and horseradish peroxidase, based on a previously described method, slightly modified (30). Fresh brain homogenates (0.3 mg) were incubated in respiration buffer containing 5 μM Amplex Red reagent and 3 units/mL horseradish peroxidase. Fluorescence was monitored at excitation and emission wavelengths of 563 nm (slit 5 nm) and 587 nm (slit 5 nm) in a Varian spectrofluorometer (Cary Eclipse Model). Calibration was performed by the addition of known quantities of H_2O_2. Succinate (10 mM) was added as the electron donor to induce state 2 respiration, leading to a polarization of $\Delta\Psi m$ and increase in H_2O_2 production. ADP (100 μM) was added to the cuvette, inducing state 3 respiration and decreasing H_2O_2 production. Oligomycin (1 μg/mL) was used to induce state 4–like respiration and FCCP (5 μM) used to induce uncoupled respiration and minimum H_2O_2 production.

Statistical Analysis. Comparisons between groups were done by the nonpaired Student's *t*-test or one-way analysis of variance, and *a posteriori* Tukey's test for pair-wise compari-

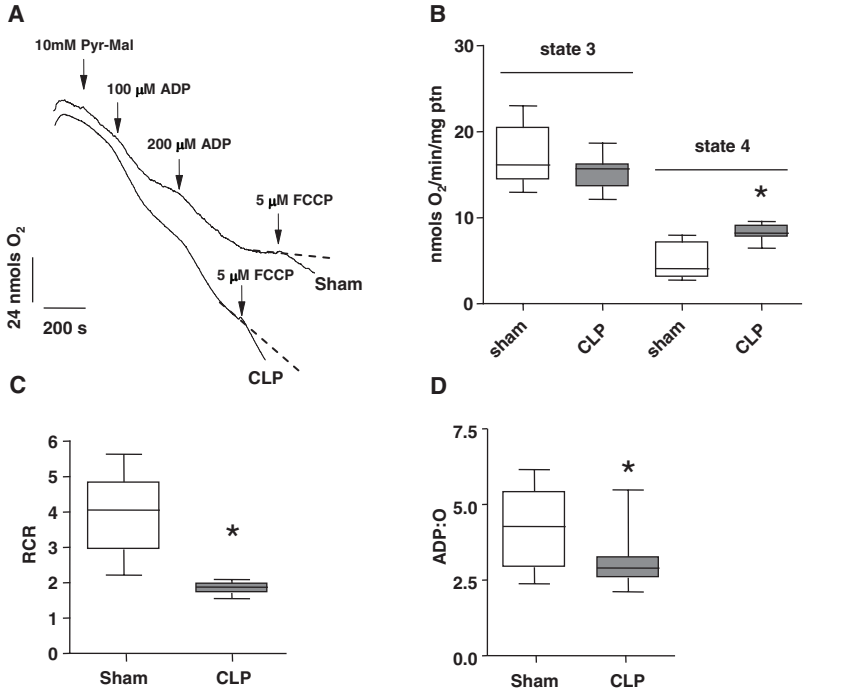

Figure 1. Sepsis-induced mitochondrial uncoupling of oxidative phosphorylation in brain homogenates. *A*, representative traces of oxygen consumption of sham and cecal ligation and perforation (*CLP*) mice, with additions as indicated. *Pyr-Mal*, pyruvate and malate; *ADP*, adenosine 5'-diphosphate; *FCCP*, carbonyl cyanide p-(trifluoromethoxy)phenylhydrazone. *Dashed lines* indicate the rate of state 4 respiration utilized for comparisons between sham and CLP samples. *B*, oxygen consumption rate of sham (n = 8, *white bars*) and CLP (n = 9, *gray bars*) animals evaluated at metabolic state 3 and state 4. Brain homogenates (650 µg/mL) were incubated at the oxygen meter cuvette with 10 mM pyruvate and malate and 100–200 µM ADP, inducing state 3 respiration. The state 4 respiration was reached in the absence of ADP (*$p < .05$ analysis of variance, Tukey's test). *C*, respiratory control ratio (*RCR*) of mitochondria from sham (n = 8, *white bars*) and CLP (n = 9, *gray bars*) mice obtained from the data presented in *A* by dividing the rate of oxygen consumption at state 3 by the rate of oxygen consumption at state 4 (*$p = .0001$, Student's *t*-test). *D*, ADP/oxygen ratio (*ADP:O*) of mitochondria from sham (n = 13, *white bars*) and CLP (n = 15, *gray bars*) mice obtained by measuring the amount of oxygen (nanomoles) consumed after addition of 0.15 mM of ADP (*$p = .03$, Student's *t*-test). Data are presented as box plots with median ± maximum and minimum values for each condition. *ptn*, protein.

sons. Differences of $p < .05$ were considered to be significant. Student's *t*-test, analysis of variance, and Tukey's test were performed by GraphPad Prism, version 4.00, for Windows (GraphPad Software, San Diego, CA).

RESULTS

Sepsis Causes Mitochondrial Uncoupling in Mice Brain. Oxygen consumption in brain homogenates was measured from sham and CLP mice in two distinct metabolic states of mitochondria: state 3, in which respiration is coupled to ATP synthesis, and state 4, which is defined as the respiration not associated to ATP synthesis (Fig. 1). Figure 1*A* shows typical traces of oxygen consumption induced by mitochondrial respiratory substrates in the two experimental groups. We observed that the oxygen consumption rate after addition of ADP (state 3) was essentially the same between the two experimental groups (Fig. 1*A*), and respiration was completely inhibited by cyanide (data not shown). However, after all of the ADP is converted to ATP, the oxygen consumption rate (state 4) was higher in CLP than in sham animals (Fig. 1*A*, *traces* indicated by *open arrowheads*). Comparison between the respiratory rates of the two metabolic states is shown in Figure 1*B*. Indeed, in septic animals, there were no significant changes in the state 3 respiration compared with sham (20.016 ± 2.52 vs. 21.456 ± 1.54 nmol oxygen·min^{-1}·mg^{-1} protein), whereas state 4 respiration was significantly higher in CLP animals compared with sham animals (12.456 ± 1.15 vs. 8.064 ± 1.58 nmol oxygen·min^{-1}·mg^{-1} protein, $p < .05$), suggesting an uncoupling of oxidative phosphorylation. The respiratory control ratio, an index of mitochondrial coupling, was significantly reduced in septic mice compared with sham animals (1.67 ± 0.11 vs. 3.3 ± 0.59) (Fig. 1*C*). An index of efficiency of oxidative phosphorylation was evaluated, the ADP/oxygen ratio, which is defined by the number of moles of ADP phosphorylated to ATP per moles of oxygen consumed (31). Brain homogenates of CLP mice exhibited a reduced ADP/oxygen ratio compared with sham (2.90 ± 0.24 vs. 4.27 ± 0.36; $p = .03$) (Fig. 1*D*). Thus, this set of data suggest that in sepsis, the proportion of oxygen used for respiration that is not associated to ATP synthesis increases in the brain as a result of an uncoupling of oxidative phosphorylation.

Sepsis Affects the Mitochondrial Membrane Potential in Mice Brain. Figure 2*A* shows typical traces of fluorescence signal of the probe safranine O when Percoll-purified mitochondria were incubated with a respiratory substrate. After addition of succinate, there was a huge decrease in safranine fluorescence in both groups because of an increase in the $\Delta\Psi m$. After the addition of ADP, the fluorescence signal of safranine increased transiently in both experimental groups because of a partial depolarization of $\Delta\Psi m$ coupled to ATP synthesis. However, the extent by which $\Delta\Psi m$ is dissipated by the same amount of ADP is different between the groups, suggesting that $\Delta\Psi m$ could be dissipated in septic brain (Fig. 2*B*). The recovery time of $\Delta\Psi m$ on ADP addition is higher in CLP mice compared with sham animals (1.509 ± 0.15 vs. 1.068 ± 0.13 secs of state 3·nmol ADP^{-1}·mg^{-1} protein), as shown in Figure 2*B*, indicating that the mechanisms that regulate $\Delta\Psi m$ and oxidative phosphorylation efficiency are affected in sepsis.

Sepsis Causes Cytochromes Depletion and Reduced Complex IV Activity. Figure 3 shows typical light absorption spectra of mitochondrial cytochromes. We observed a reduction of cytochrome *b* (near 560 nm), cytochrome *c* (near 551 nm), and cytochrome $a+a_3$ (near 604 nm) absorption in septic animals, indicating that in sepsis, there is a depletion of the content of cytochromes. To check if the reduction in cytochromes content would affect mitochondrial electron transfer, we determined the activity of Complexes I–III and Complex IV (Fig. 4). In our experimental conditions, we did not detect differences in the activities of Complexes I–III during sepsis (sham, 26.35 ± 3.24 nmol cytochrome *c*·min^{-1}·mg^{-1} protein; CLP, 24.00 ± 0.49 nmol cytochrome *c*·min^{-1}·mg^{-1} protein) (Fig. 4*A*). On the other hand, there was a clear inhibition in Complex IV activity in the

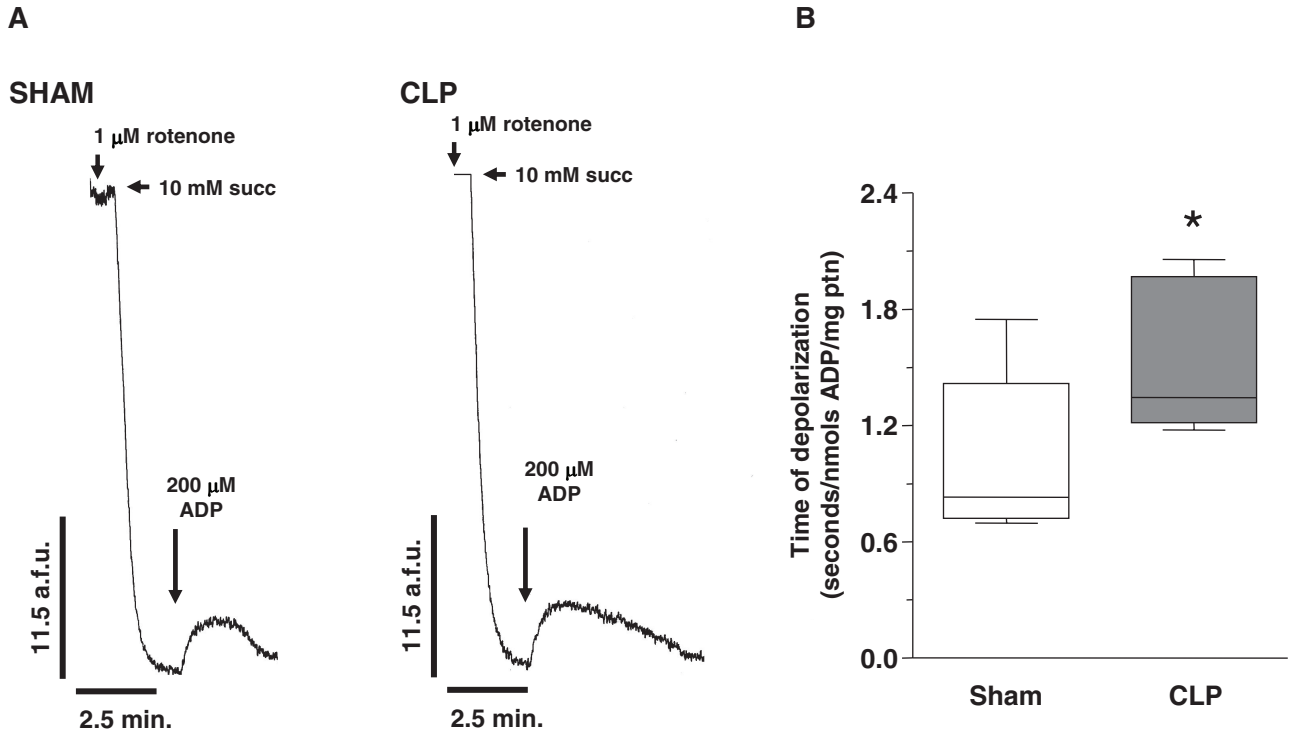

Figure 2. Sepsis induced changes in mitochondrial membrane potential ($\Delta\Psi m$). *A*, traces of safranine O fluorescence of Percoll-purified brain mitochondria from sham and cecal ligation and perforation (*CLP*) mice. Brain mitochondria (200 μg/mL) were incubated at the fluorometer cuvette with 10 mM succinate (*succ*) and 1 μM rotenone, inducing state 2 respiration. Sequential addition of adenosine 5'-diphosphate (*ADP*, 0.2 mM) was made to induce a transient state 3 respiration and partial $\Delta\Psi$m dissipation. *B*, the time of state 3 respiration induced by ADP was measured in brain mitochondria from sham (n = 9, *white bars*) and CLP (n = 6, *gray bars*) animals (*$p < .01$, Student's *t*-test). Data are presented as box plots with median ± maximum and minimum values for each condition. *a.f.u.*, arbitrary fluorescence units; *ptn*, protein.

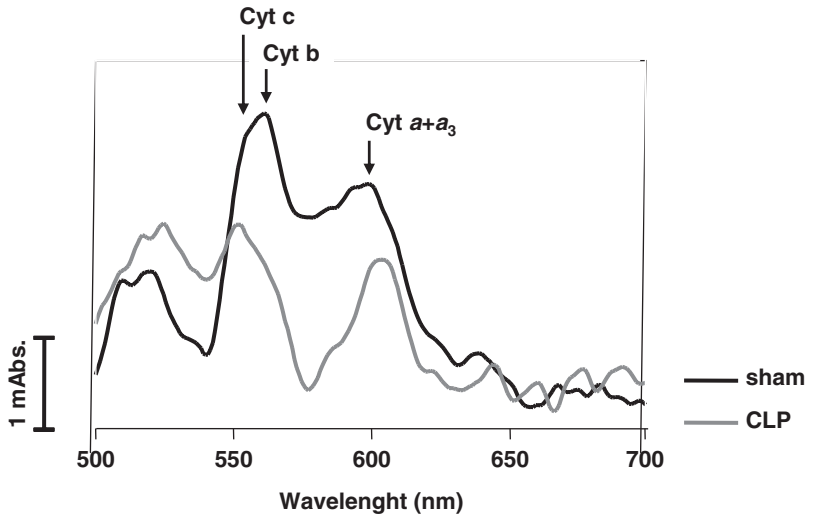

Figure 3. Sepsis-promoted depletion of mitochondrial cytochromes (*Cyt*). Representative absorption light differential spectra of brain homogenates from sham (*black line*) and cecal ligation and perforation (*CLP*; *gray line*) mice are shown.

CLP group compared with sham (31.80 ± 1.55 vs. 40.45 ± 3.31 nmol oxygen·min^{-1}·mg^{-1} protein) (Fig. 4*B*).

Mitochondrial Hydrogen Peroxide Generation in Septic Brain Is Reduced. Figure 5*A* shows typical traces of mitochondrial H_2O_2 production both in sham and CLP brains. We observed that basal H_2O_2 production (state 1) was not different between the experimental groups. In brains from sham animals, succinate addition stimulated the H_2O_2 formation because of an increase in membrane potential in a nonphosphorylating condition (state 2) (Fig. 5*B*). As expected, ADP-induced state 3 respiration inhibited H_2O_2 formation in brains from sham animals (Fig. 5*B*) because of dissipation of membrane potential through ATP synthase activity. Interestingly, we observed that in brains from CLP mice, H_2O_2 production was not stimulated by succinate addition (Fig. 5*B*). We also observed that oligomycin-induced state 4–like respiration failed to induce H_2O_2 generation in CLP mice, suggesting that uncoupling of oxidative phosphorylation impairs the maintenance of membrane potential, which in turn reduces H_2O_2 production (Fig. 5*B*).

DISCUSSION

Several lines of evidence indicate a critical role of mitochondrial dysfunction in the pathogenesis both of acute and chronic diseases in the brain (20). Despite the recent efforts to understand the involvement of mitochondria in the development of brain diseases, a systematic survey of mitochondrial function in brain tissues during sepsis is lacking. The present article is the first demonstration

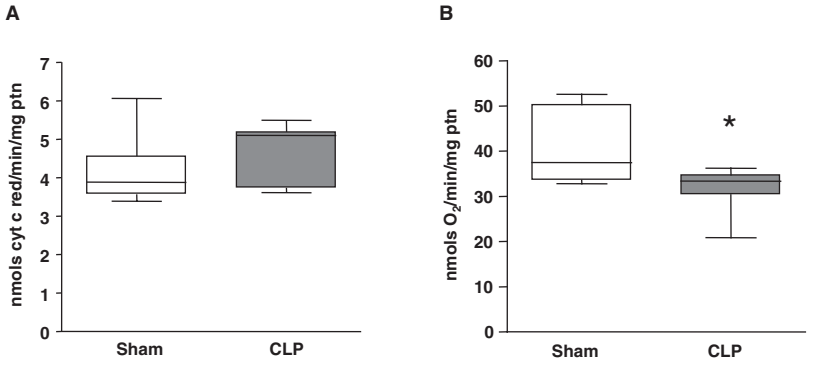

Figure 4. Inhibition of cytochrome *c* oxidase in sepsis. *A*, activity of Complexes I–III from mitochondrial electron transport chain were evaluated in brain homogenates (0.35 mg/mL) from sham (n = 11, *white bars*) and cecal ligation and perforation (*CLP*; n = 9, *gray bars*) mice by measuring the absorbance at 550 nm of cytochrome *c* (0.05 mM) reduction (*cyt c red*) induced by reduced nicotinamide adenine dinucleotide (0.2 mM) inhibited by rotenone (2 μM). All of the measurements were made in the presence of 1 mM potassium cyanide. *B*, activity of cytochrome *c* oxidase from mitochondrial electron transport chain was evaluated in brain homogenates (0.2–0.4 mg/mL) from sham (n = 6, *white bars*) and CLP (n = 9, *gray bars*) mice by measuring the oxygen consumption induced by 0.5 mM tetramethylparaphenylinediamine and 5 mM ascorbate and inhibited by 1 mM potassium cyanide (*p = .02, Student's t-test). Data are presented as box plots with median ± maximum and minimum values for each condition. *ptn*, protein.

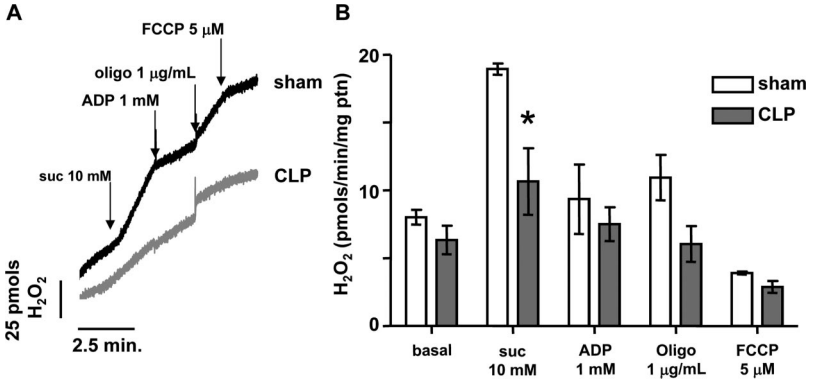

Figure 5. Hydrogen peroxide (H_2O_2) formation in brain homogenates from septic mice is not regulated by respiratory substrate and adenosine 5'-diphosphate (*ADP*). *A*, representative traces of H_2O_2 formation in brain homogenates (0.2 mg/mL) from sham (*black line*) and cecal ligation and perforation (*CLP*; *gray line*) mice were assessed fluorometrically through the oxidation of the probe Amplex Red (2 μM) induced by succinate (*suc*, 10 mM). State 3 respiration was induced by addition of 1 mM ADP and state 4–like respiration was induced by 2 μg/mL oligomycin (*oligo*). Carbonyl cyanide p-(trifluoromethoxy)phenylhydrazone (*FCCP*, 5 μM) was added to evaluate H_2O_2 generation during the uncoupled state. *B*, H_2O_2 generation in four metabolic states of mitochondria was evaluated in brain homogenates of sham (n = 3, *white bars*) and CLP (n = 3, *gray bars*) mice (*p = .03, Student's t-test). *Bars* represent mean ± SEM, and similar results were obtained with preparations from different animals. *ptn*, protein.

of mitochondrial dysfunction in the brain during sepsis, showing changes in oxygen consumption, mitochondrial complex activities, contents of cytochromes, membrane potential, and H_2O_2 generation. The data presented here are schematically summarized in Figure 6. The changes in brain mitochondrial function observed in our model of sepsis were essentially related to an increase in proton permeability across the inner mitochondrial membrane, leading to a reduction of oxidative phosphorylation efficiency due to mitochondrial uncoupling (Figs. 1, 2, and 5). This can be proposed based on an increase in oxygen consumption during state 4 respiration (Fig. 1), increased time of depolarization of ΔΨm induced by ADP (Fig. 2), and also by the reduced capacity of mitochondria to generate H_2O_2 after induction by respiratory substrates (Fig. 5). Supporting these observations, an increase in the state 4 respiration and a reduction in ADP/oxygen ratio were also demonstrated by other groups in the liver (10, 32, 33) and in the diaphragm (34) during endotoxemia. We observed changes in the ΔΨm after ADP addition, and the time of repolarization of ΔΨm was significantly increased in CLP animals, suggesting an increase of proton permeability across the inner mitochondrial membrane, even during state 3 (Fig. 2). In agreement with these data, the ADP/oxygen ratio in the septic brain presented a significant reduction, indicating that, despite not affecting the rate of oxygen consumption during state 3 respiration, the increase in proton permeability during state 3 respiration induced by sepsis affects the efficiency of oxidative phosphorylation (Fig. 1*D*). It is important to note that a loss of ΔΨm has been shown to be directly associated to processes such as mitochondrial permeability transition (MPT), mitochondrial swelling, and apoptosis (35). Moreover, Adrie et al. (8) have shown in peripheral blood monocytes of septic patients both a loss of ΔΨm and the appearance of apoptosis markers, which were related to the severity of sepsis.

The inhibition of the electron transport, particularly at the Complex I site, is a hallmark of mitochondrial dysfunction in sepsis (9, 36), and inhibition of Complex IV has also been detected in some studies (37, 38). The impairment of the electron flux in mitochondria results in a reduction in oxygen utilization, which was hypothesized as the *cytopathic hypoxia* concept (39). However, the data presented here indicate that electron transport chain function is maintained in the septic brain, despite many reports showing inhibition of state 3 respiration or inhibition of complex activities in different tissues (9, 10, 32, 37). Indeed, we did not find inhibition of Complex I activity but, instead, a reduction of approximately 30% of Complex IV activity (Fig. 4). This inhibition of Complex IV could involve mediators such as nitric oxide (40) and carbon monoxide (41). Interestingly, Brealey et al. (9) established an association between Complex I inhibition and sepsis severity. They also found a direct correlation between the levels of nitric oxide metabolites and Complex I inhibition, which may be mediated by peroxynitrite (28, 42). The literature has shown that the involvement of nitric oxide or peroxynitrite, or both, on Complex I activity seems to be different in the brain compared with other tissues (40). There is a general consensus that one of the protective components against oxidative damage of Complex I is the presence of reduced glutathione, an endogenous an-

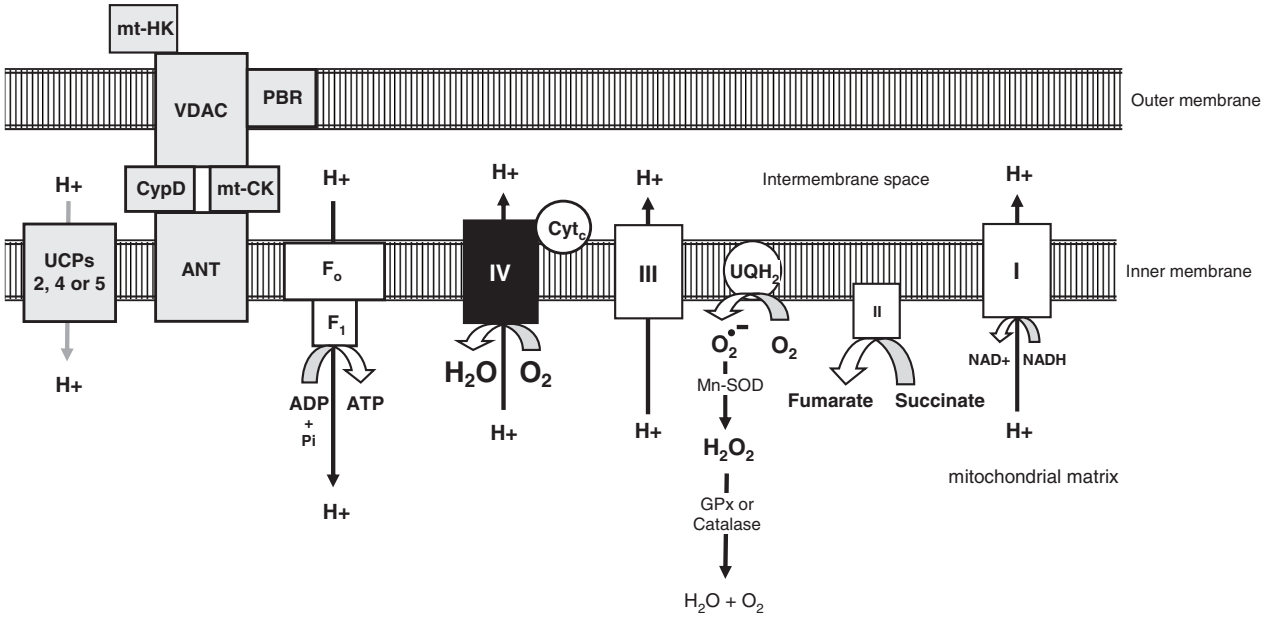

Figure 6. Schematic representation of the proposed mechanisms by which sepsis induces brain mitochondrial dysfunction. The *boxes* represent mitochondrial proteins and the *hatched rectangles* the inner and outer mitochondrial membranes. The boxes' colors are indicative of their involvement in septic brain: *white* is not affected, *gray* is possibly affected, and *black* is affected. The complexes of the electron transport chain generate a proton (H^+) gradient across the inner mitochondrial membrane using the oxygen as an electron sink. It is possible that proteins involved in the maintenance of the membrane potential ($\Delta\Psi m$) would be affected during sepsis. In the brain and other tissues, hexokinase (*HK*) is bound to the outer mitochondrial membrane through an association with the voltage-dependent anion channel (*VDAC*). The octameric form of mitochondrial creatine kinase (*mt-CK*) localizes in the intermembrane space, through an association with the VDAC and the adenine nucleotide translocator (*ANT*) and with cyclophilin D (*CypD*) and the peripheral benzodiazepine receptor (*PBR*). *Open arrows* and *black lines* indicate a high flux of metabolites, whereas *gray lines* represent low flux. *Numbers* represent the complexes of the respiratory electron chain. *UQ*, ubiquinone; *Cyt c*, cytochrome *c*; *UCP-2*, *UCP-4*, or *UCP-5*, uncoupling protein isoforms 2, 4, or 5; *Mn-SOD*, manganese superoxide dismutase; *GPx*, glutathione peroxidase; F_1F_o, F_1F_o-adenosine triphosphate (*ATP*) synthase; *NAD+*, oxidized nicotinamide adenine dinucleotide; *NADH*, reduced nicotinamide adenine dinucleotide; *Pi*, inorganic phosphate.

tioxidant molecule that is particularly important in brain physiology (43). In fact, brain glutathione metabolism is essential to maintain mitochondrial electron transport chain complex activities (44–46). Whatever the mechanism, Kadoi and Goto (47) have shown that nitric oxide synthase inhibitors restored hemodynamic changes but did not lead to an improvement of septic encephalopathy. Therefore, Complex I inhibition may not be of central importance to the development of brain mitochondrial uncoupling (Figs. 5 and 6). The overall picture of mitochondrial dysfunctions in sepsis is complex, and sometimes, the conclusions established go in opposite directions. Possibly, much of this controversy can be associated with factors such as differences in experimental settings and choice of the model, the tissue, or time of disease progression.

Despite a reduction in cytochrome levels observed in the septic brain (Fig. 3), an impairment of complex activities was only detected at the cytochrome *c* oxidase level (Fig. 4). Interestingly, depletion of cytochromes was also observed in other tissues during sepsis (48). Thus, it seems that cytochrome depletion, in our model, was not enough to compromise the electron flux in septic brain mitochondria, but the mechanisms underlying this process are not known. A biochemical threshold effect could explain why depletion of cytochromes occurs without any apparent effect on electron flux during state 3 respiration (49, 50).

Mechanistically, we can speculate about the pathways involved in the uncoupling of oxidative phosphorylation observed in our model of sepsis in brain. The activation of uncoupling proteins (UCPs) or the opening of mitochondrial permeability transition pores would result in a reduction of $\Delta\Psi m$, leading to an inefficiency of oxidative phosphorylation. In this regard, the early oxidative stress condition, observed in previous studies of the septic brain (19), could be responsible for the uncoupling of oxidative phosphorylation observed here, through the activation of UCP. Echtay et al. (51, 52) have shown that superoxide radical and 4-hydroxynonenal, a product of lipid peroxidation, are both able to activate UCP. Thus, it is tempting to propose that in early sepsis, products of lipid peroxidation might accumulate to levels that would activate brain isoforms of UCP, increasing the proton permeability across the inner mitochondrial membrane. Interestingly, Sun et al. (53) have recently demonstrated that UCP-3 expression was increased in the muscle of CLP rats and, although brain essentially expresses UCPs 2, 4, and 5 instead of UCP-3, it is conceivable that expression of other UCP isoforms in brain would be increased. Thus, UCP activation could explain the increase in oxygen consumption in state 4 (Fig. 1), the reduced respiratory control and the ADP/oxygen ratios (Fig. 1), and the reduction in H_2O_2 generation (Fig. 5) (51, 52). However, we cannot exclude the possibility of an altered proton permeability mediated by other mechanisms independent of UCP, such as the opening of the mitochondrial permeability transition pore. Regardless of the mechanisms involved in mitochondrial uncoupling, it is important to note that mitochondrial reactive oxygen species production is dependent on the $\Delta\Psi m$ in such a way that small changes in membrane potential could result in drastic changes in H_2O_2 production (54, 55).

Despite the interesting findings presented here, we are aware that the observed effects in brain mitochondria during sepsis were detected in whole homogenates, and it is not possible to determine whether mitochondrial uncoupling occurs diffusely or is restricted to specific areas of the brain. In addition, we have no information about which cell types are affected during sepsis. Finally, although an encephalopathy of variable severity is present in septic patients, it is not clear what the relationship between mitochondrial dysfunction and the degree of cognitive or motor impairment is during sepsis. Experiments directed to investigate these issues in murine models are currently under way in our laboratory.

Taken together, the results presented here show that brain mitochondrial function is affected during sepsis due to an increase in proton permeability of the inner membrane, leading to a reduction in oxidative phosphorylation efficiency. Further studies under way are aimed to establish the early events that lead to a lower oxidative phosphorylation efficiency in the brain during sepsis. Once confirmed in a clinical setting, changes in brain energy metabolism resulting from mitochondrial dysfunctions may represent a new mechanism for understanding septic encephalopathy and may become an emerging target for the development of therapies for this condition.

CONCLUSIONS

Mitochondrial dysfunction is present in brain tissue during sepsis and is characterized by an uncoupling of oxidative phosphorylation, which may compromise the tissue bioenergetic efficiency.

ACKNOWLEDGMENTS

We thank Dr. Hugo Castro-Faria-Neto and Ms. Juliette Savin for critical revision of the manuscript and Andrew S. Weyrich and Guy A. Zimmerman for critical review of the manuscript.

REFERENCES

1. Fink MP, Evans TW: Mechanisms of organ dysfunction in critical illness: Report from a Round Table Conference held in Brussels. *Intensive Care Med* 2002; 28:369–375
2. Gattinoni L, Brazzi L, Pelosi P, et al: A trial of goal-oriented hemodynamic therapy in critically ill patients: SvO_2 Collaborative Group. *N Engl J Med* 1995; 333:1025–1032
3. Hayes MA, Timmins AC, Yau EH, et al: Oxygen transport patterns in patients with sepsis syndrome or septic shock: Influence of treatment and relationship to outcome. *Crit Care Med* 1997; 25:926–936
4. Kern JW, Shoemaker WC: Meta-analysis of hemodynamic optimization in high-risk patients. *Crit Care Med* 2002; 30:1686–1692
5. Rivers E, Nguyen B, Havstad S, et al: Early goal-directed therapy in the treatment of severe sepsis and septic shock. *N Engl J Med* 2001; 345:1368–1377
6. Crouser ED: Mitochondrial dysfunction in septic shock and multiple organ dysfunction syndromes. *Mitochondrion* 2004; 4:729–741
7. Protti A, Singer M: Bench-to-bedside review: Potential strategies to protect or reverse mitochondrial dysfunction in sepsis-induced organ failure. *Crit Care* 2006; 10:228
8. Adrie C, Bachelet M, Vayssier-Taussat M, et al: Mitochondrial membrane potential and apoptosis peripheral blood monocytes in severe human sepsis. *Am J Respir Crit Care Med* 2001; 164:389–395
9. Brealey D, Brand M, Hargreaves I, et al: Association between mitochondrial dysfunction and severity and outcome of septic shock. *Lancet* 2002; 360:219–223
10. Crouser ED, Julian MW, Blaho DV, et al: Endotoxin-induced mitochondrial damage correlates with impaired respiratory activity. *Crit Care Med* 2002; 30:276–284
11. Porta F, Takala J, Weikert C, et al: Effects of prolonged endotoxemia on liver, skeletal muscle and kidney mitochondrial function. *Crit Care* 2006; 10:R118
12. Lin MT, Beal MF: Mitochondrial dysfunction and oxidative stress in neurodegenerative diseases. *Nature* 2006; 443:787–795
13. Milbrandt EB, Angus DC: Bench-to-bedside review: Critical illness-associated cognitive dysfunction-mechanisms, markers, and emerging therapeutics. *Crit Care* 2006; 10: 238
14. Ebersoldt M, Sharshar T, Annane D: Sepsis-associated delirium. *Intensive Care Med* 2007; 33:941–950
15. Sprung CL, Peduzzi PN, Shatney CH, et al: Impact of encephalopathy on mortality in the sepsis syndrome: The Veterans Administration Systemic Sepsis Cooperative Study Group. *Crit Care Med* 1990; 18:801–806
16. Eidelman LA, Putterman D, Putterman C, et al: The spectrum of septic encephalopathy: Definitions, etiologies, and mortalities. *JAMA* 1996; 275:470–473
17. Sharshar T, Annane D, de la Grandmaison GL, et al: The neuropathology of septic shock. *Brain Pathol* 2004; 14:21–33
18. Barichello T, Martins MR, Reinke A, et al: Cognitive impairment in sepsis survivors from cecal ligation and perforation. *Crit Care Med* 2005; 33:221–223
19. Barichello T, Fortunato JJ, Vitali AM, et al: Oxidative variables in the rat brain after sepsis induced by cecal ligation and perforation. *Crit Care Med* 2006; 34:886–889
20. Halliwell B: Oxidative stress and neurodegeneration: Where are we now? *J Neurochem* 2006; 97:1634–1658
21. Baker CC, Chaudry IH, Gaines HO, et al: Evaluation of factors affecting mortality rate after sepsis in a murine cecal ligation and puncture model. *Surgery* 1983; 94:331–335
22. Vianna RC, Gomes RN, Bozza FA, et al: Antibiotic treatment in a murine model of sepsis: Impact on cytokines and endotoxin release. *Shock* 2004; 21:115–120
23. Sims NR, Blass JP: Expression of classical mitochondrial respiratory responses in homogenates of rat forebrain. *J Neurochem* 1986; 47:496–505
24. Lowry OH, Rosebrough NJ, Farr AL, et al: Protein measurement with the Folin phenol reagent. *J Biol Chem* 1951; 193:265–275
25. Sims NR: Rapid isolation of metabolically active mitochondria from rat brain and subregions using Percoll density gradient centrifugation. *J Neurochem* 1990; 55:698–707
26. Chance B, Williams GR: Respiratory enzymes in oxidative phosphorylation: I. Kinetics of oxygen utilization. *J Biol Chem* 1955; 217: 383–393
27. Akerman KE, Wikstrom MK: Safranine as a probe of the mitochondrial membrane potential. *FEBS Lett* 1976; 68:191–197
28. Cassina A, Radi R: Differential inhibitory action of nitric oxide and peroxynitrite on mitochondrial electron transport. *Arch Biochem Biophys* 1996; 328:309–316
29. Navarro A, Boveris A: Rat brain and liver mitochondria develop oxidative stress and lose enzymatic activities on aging. *Am J Physiol Regul Integr Comp Physiol* 2004; 287:R1244–R1249
30. Votyakova TV, Reynolds IJ: Detection of hydrogen peroxide with Amplex Red: Interference by NADH and reduced glutathione autooxidation. *Arch Biochem Biophys* 2004; 431: 138–144
31. Nicholls DG, Ferguson SJ: Bioenergetics 3. Third Edition. London, Academic Press, 2002
32. Schumer W, Das Gupta TK, Moss GS, et al: Effect of endotoxemia on liver cell mitochondria in man. *Ann Surg* 1970; 171:875–882
33. Porta F, Takala J, Weikert C, et al: Effect of endotoxin, dobutamine and dopamine on muscle mitochondrial respiration in vitro. *J Endotoxin Res* 2006; 12:358–366
34. Boczkowski J, Lisdero CL, Lanone S, et al: Endogenous peroxynitrite mediates mitochondrial dysfunction in rat diaphragm during endotoxemia. *FASEB J* 1999; 13: 1637–1646
35. Kowaltowski AJ, Castilho RF, Vercesi AE: Mitochondrial permeability transition and oxidative stress. *FEBS Lett* 2001; 495:12–15
36. Brealey D, Karyampudi S, Jacques TS, et al: Mitochondrial dysfunction in a long-term rodent model of sepsis and organ failure. *Am J Physiol Regul Integr Comp Physiol* 2004; 286:R491–R497
37. Chuang YC, Tsai JL, Chang AY, et al: Dysfunction of the mitochondrial respiratory chain in the rostral ventrolateral medulla

during experimental endotoxemia in the rat. *J Biomed Sci* 2002; 9:542–548
38. Vanhorebeek I, De Vos R, Mesotten D, et al: Protection of hepatocyte mitochondrial ultrastructure and function by strict blood glucose control with insulin in critically ill patients. *Lancet* 2005; 365:53–59
39. Fink MP: Cytopathic hypoxia: Mitochondrial dysfunction as mechanism contributing to organ dysfunction in sepsis. *Crit Care Clin* 2001; 17:219–237
40. Moncada S, Bolanos JP: Nitric oxide, cell bioenergetics and neurodegeneration. *J Neurochem* 2006; 97:1676–1689
41. D'Amico G, Lam F, Hagen T, et al: Inhibition of cellular respiration by endogenously produced carbon monoxide. *J Cell Sci* 2006; 119: 2291–2298
42. Riobo NA, Clementi E, Melani M, et al: Nitric oxide inhibits mitochondrial NADH:ubiquinone reductase activity through peroxynitrite formation. *Biochem J* 2001; 359: 139–145
43. Clementi E, Brown GC, Feelisch M, et al: Persistent inhibition of cell respiration by nitric oxide: Crucial role of S-nitrosylation of mitochondrial complex I and protective action of glutathione. *Proc Nat Acad Sci U S A* 1998; 95:7631–7636
44. Barker JE, Heales SJ, Cassidy A, et al: Depletion of brain glutathione results in a decrease of glutathione reductase activity, an enzyme susceptible to oxidative damage. *Brain Res* 1996; 716:118–122
45. Bolanos JP, Heales SJ, Peuchen S, et al: Nitric oxide-mediated mitochondrial damage: A potential neuroprotective role for glutathione. *Free Radic Biol Med* 1996; 21:995–1001
46. Gegg ME, Beltran B, Salas-Pino S, et al: Differential effect of nitric oxide on glutathione metabolism and mitochondrial function in astrocytes and neurones: Implications for neuroprotection/neurodegeneration? *J Neurochem* 2003; 86:228–237
47. Kadoi Y, Goto F: Selective inducible nitric oxide inhibition can restore hemodynamics, but does not improve neurological dysfunction in experimentally-induced septic shock in rats. *Anesth Analg* 2004; 99:212–220
48. Callahan LA, Supinski GS: Sepsis induces diaphragm electron transport chain dysfunction and protein depletion. *Am J Respir Crit Care Med* 2005; 172:861–868
49. Letellier T, Heinrich R, Malgat M, et al: The kinetic basis of threshold effects observed in mitochondrial diseases: A systemic approach. *Biochem J* 1994; 302(Pt 1):171–174
50. Gnaiger E, Lassnig B, Kuznetsov A, et al: Mitochondrial oxygen affinity, respiratory flux control and excess capacity of cytochrome *c* oxidase. *J Exp Biol* 1998; 201: 1129–1139
51. Echtay KS, Roussel D, St-Pierre J, et al: Superoxide activates mitochondrial uncoupling proteins. *Nature* 2002; 415:96–99
52. Echtay KS, Esteves TC, Pakay JL, et al: A signalling role for 4-hydroxy-2-nonenal in regulation of mitochondrial uncoupling. *EMBO J* 2003; 22:4103–4110
53. Sun X, Wray C, Tian X, et al: Expression of uncoupling protein 3 is upregulated in skeletal muscle during sepsis. *Am J Physiol Endocrinol Metab* 2003; 285:E512–E520
54. Boveris A, Chance B: The mitochondrial generation of hydrogen peroxide: General properties and effect of hyperbaric oxygen. *Biochem J* 1973; 134:707–716
55. Korshunov SS, Skulachev VP, Starkov AA: High protonic potential actuates a mechanism of production of reactive oxygen species in mitochondria. *FEBS Lett* 1997; 416: 15–18